BOUNDARY SCATTERING OF ELECTRONS IN THIN

CADMIUM SINGLE CRYSTALS

APPROVED:

H J Mackey
Major Professor

J. W. Kauffman
Minor Professor

L. F. Bonnell Jr.
Director of the Department of Physics

Robert B. Toulouse
Dean of the Graduate School

BOUNDARY SCATTERING OF ELECTRONS IN THIN CADMIUM SINGLE CRYSTALS

THESIS

Presented to the Graduate Council of the North Texas State University in Partial Fulfillment of the Requirements

For the Degree of

MASTER OF SCIENCE

By

Gary William Fortmayer, B.S.

Denton, Texas

August, 1968

TABLE OF CONTENTS

LIST OF ILLUSTRATIONS

CHAPTER I

INTRODUCTION

In thin metal films where the mean free path is on the order of the dimensions of the sample, one must consider the effects of boundary scattering in problems of electron transport.

Sondheimer (4) has treated the case of conductivity in thin samples with a transverse magnetic field. In particular, he predicted oscillations in the Hall effect and transverse magnetoresistance as a function of magnetic field with the magnetic field applied perpendicular to the plane of a thin conducting plate.

In 1963, large-amplitude oscillations periodic in the magnetic field were found in the Hall resistivity of cadmium single crystals at liquid-helium temperatures by Zebouni, Hamburg, and Mackey (5). Oscillations of the same period and comparable amplitude were also observed in the transverse magnetoresistivity. These phenomena appeared to be the size-effect oscillations predicted by Sondheimer.

Mackey, Sybert, and Fielder (1) observed oscillations in the Hall resistivity in a monocrystal of highly pure cadmium at liquid-helium temperatures with the magnetic field parallel to the hexagonal axis, which was perpendicular to

the large face of the thin sample used. The dependence on thickness parallel to the magnetic field was studied in the period, phase, and amplitude of the oscillations. It was concluded that the lens-shaped pocket of electrons, which occurs in the third Brillouin zone of cadmium, was responsible for the observed oscillations.

Attempts to observe short-period oscillations observed by other researchers (1) failed. During this search, it was found that the amplitude of the size-effect oscillations was larger if the surface of the crystal had a spark-planed finish rather than an electropolished finish. The signal could also be enhanced if the electropolished surface were abraded with fine emery cloth. This enhancement in aplitude implied that an appreciable number of electrons scatter specularly at an electropolished surface, since only diffusely scattered electrons can contribute to the size-effect oscillations. It was suggested that a very thin distorted layer at the crystal surface may be necessary to observe the short-period oscillations.

Mackey and Sybert (2) have treated the effect of partially specular boundary scattering upon the magneto-oscillatory component of the kinetic coefficients for the case of Fermi surfaces which are figures of revolution about the normal to the plane of a thin crystal, with magnetic field directed along the normal. It was shown that the oscillations consisted of the superposition of a fundamental

and all its harmonics. Explicit expressions were given for the amplitude dependence upon the fraction of electrons which scattered specularly. In particular, it was shown that only the fundamental was present for the case of completely diffuse scattering, in which scattering angle is independent of angle of incidence.

Mackey and Sybert (3) have also considered the oscillatory components of the kinetic coefficients of electron transport due to scattering from two crystalline surfaces described by distinct scattering parameters for the case of Fermi surfaces which are surfaces of revolution about the normal to a thin crystal with magnetic field directed along the symmetry axis. Explicit expressions were derived for the dependence of the amplitudes of the various harmonics which arise upon the scattering parameters. The amplitudes of the harmonics were predicted to be very small as compared to the amplitude of the fundamental size-effect oscillation. For this reason, detection had not been possible to that time.

Based on the previously obtained results of Fielder (1) it was hoped that a suitable method for increasing the diffuse scattering at one of the surfaces could be found and that this technique could be used to detect the higher harmonics of the size-effect oscillation by controlling the scattering parameters at each surface of a crystal of cadmium.

In the present investigation, zinc was plated onto a cadmium crystal to determine the effect on the scattering parameter. Measurements of the size-effect oscillation were performed with respect to amplitude and period as a function of the angle between the magnetic field and the crystal normal. The effect of varying thicknesses of zinc plating on one of the crystal surfaces was studied and a search for the second harmonic of the size-effect oscillation was undertaken.

The equation of the Fermi surface in the third Brillouin zone is calculated from a perturbation equation developed by Ziman. From this equation the Gaussian radius of curvature is calculated for points on the Fermi surface between plus ninety and minus ninety degrees as measured from the normal to the crystal. Measurements are made of the period of the size-effect oscillations between plus twelve and one-half degrees and minus sixteen degrees and the experimental values of the Gaussian radius of curvature are calculated and are compared with the theoretical values.

CHAPTER BIBLIOGRAPHY

1. Mackey, H. J., J. R. Sybert, and J. T. Fielder, "Effect of Sample Geometry on Magnetomorphic Oscillations in the Hall Effect in Cadmium at Liquid-Helium Temperatures," Physical Review, CLVII (May, 1967), 578-585.

2. Mackey, H. J. and J. R. Sybert, "Harmonic Content of Magnetomorphic Oscillations in the Kinetic Coefficients of Electron Transport due to Partially Specular Boundary Scattering," Physical Review, CLVIII (June, 1967), 658-661.

3. Mackey, H. J. and J. R. Sybert, "Magnetomorphic Oscillations in Crystals with Two Surface-Scattering Parameters," Physical Review, CLXIV (December, 1967), 982-984.

4. Sondheimer, E. H., "The Influence of a Transverse Magnetic Field on the Conductivity of Thin Metallic Films," Physical Review, LXXX (November, 1950), 401-406.

5. Zebouni, N. H., R. E. Hamburg, and H. J. Mackey, "Magnetomorphic Oscillations in the Hall Effect and Magnetoresistance in Cadmium," Physical Review Letters, XI (September, 1963), 260-264.

CHAPTER II

EXPERIMENTAL PROCEDURE

The orientation of the hexagonal axis of a crystal in an ingot of 69-grade cadmium obtained from Cominco Products, Inc., Spokane, Washington was determined by means of Laue photographs taken with the aid of a Norelco X-ray generator equipped with a Polaroid XR-7 cassette.

The crystal was separated from the ingot and attached to a special goniometer, which was fitted to the X-ray generator. A series of Laue diffraction photographs was taken at twenty kilovolts and twenty milliamperes. (Higher voltages resulted in fogging of the film and the indicated current gave suitably bright photographs in five minutes.) The crystal was oriented by means of the Laue photographs so that the X-ray beam was parallel to the hexagonal axis. Once the goniometer was adjusted so that the X-ray beam was directed down the hexagonal axis of the crystal, the goniometer was locked down in that position and removed from the X-ray generator.

The goniometer was mounted onto a Servomet Spark Machine manufactured by Metals Research Ltd., Cambridge, England and the crystal was planed by means of a spark-planing wheel to establish a reference surface. The crystal was then removed

and cemented onto the goniometer with the reference surface against the goniometer surface. The goniometer was set on (0,0) and another Laue photograph was taken to check the orientation of the crystal. In this manner, the X-ray beam and the hexagonal axis of the crystal were made parallel within one degree. With this particular geometry, the large face of the crystal was perpendicular to the hexagonal axis of the crystal.

The other surface was spark planed using a coarse setting until a suitably large flat area was present on both sides of the crystal. Once the surface area was large enough, the sides of the crystal were trimmed into the form of a rectangular parallelepiped using 16-gauge flat brass strips and a medium cut. From this large parallelepiped, several smaller parallelepipeds were cut. One of the several parallelepipeds was selected to be processed into the finished crystal. To obtain a finished crystal, it was necessary to spark plane the crystal to a thickness of approximately 0.75 millimeter by means of the brass planing wheel.

The Servomet has seven cutting settings which range from one to seven. The higher the number, the finer the cutting action and the closer the wheel must work to the surface of the crystal. When the setting of six is used, the wheel is so close to the surface of the crystal that it will strike the crystal if the crystal surface and the surface of the

wheel are not exactly parallel. For this reason, the finest of the seven settings cannot normally be employed and the setting of six must be used with a special technique.

In order to minimize the sub-surface damage due to spark planing, each side of the crystal was planed while going to systematically finer cutting settings. Once the cutting setting of five was completed on each side of the crystal, the specialized technique had to be employed.

To insure that the wheel was parallel to the surface of the crystal, the wheel was first finished with a surface grinder. The wheel was then allowed to plane into an aluminum jig on the five setting until the jig's surface and the surface of the wheel were judged to be parallel. The crystal was then cemented with model airplane cement to the surface of the jig, and the wheel was allowed to plane into each of the two surfaces in turn while on the six setting. When the crystal was judged to be of the proper thickness by means of a dial indicator on the machine, it was removed from the jig to be cleaned. The crystal was washed with trichlorethylene to remove the cutting oil. A dark film on the crystal, which was formed by the spark-planing process, was removed by soaking in a solution of warm chromic acid.

Once the crystal was prepared, a series of Laue X-ray diffraction photographs were taken and the large surfaces were found to be parallel to each other to with one degree. The dimensions of the crystal were precisely measured with

the aid of a Unitron depthscope equipped with x-y translation drums calibrated directly in microns and a z translation calibrated to five microns. The final crystal was 19.514 millimeters long, 10.833 millimeters wide, and 0.746 millimeters thick.

Current, magnetoresistance, and Hall leads were soldered onto one of the six-cut crystal faces using Cerroseal-35 solder and Salmet flux. The lead wires were selected from a lot of #34 copper wire as this size wire is very easy to solder and holds up well under experimental stresses.

Due to the heat-conduction properties of cadmium, all the leads had to be soldered to the crystal at the same time. The ends of the wires were tinned and given a small lump of solder. A small amount of Salmet flux was then placed on the end of each solder lump. The wires were all fastened in a jig to hold them in their proper orientation and were lowered by means of a large x-y-z translation goniometer until they were in firm contact with the crystal, which was placed on a hot plate. The heat was turned on until the solder just melted. When this happened, the heat was turned off and the hot plate and crystal were allowed to cool for several hours. The wires were then tested to be sure they were frimly attached. The exact distance between the probes was measured on the Unitron depthscope and the information recorded for future use.

The lead wires were twisted in pairs to minimize magnetic pick-up and were attached at the base of the crystal holder to wires that went out of the Dewar system via a pair of vacuum-tight lead-in fittings.

The wires that led out of the Dewar were twisted in pairs and were wrapped in an insulating material and then placed inside shielding to prevent electrical interference. The current wires were brought out of the Dewar through a separate lead-in to prevent variations in the current forming a signal in the other wires.

The junctions where the crystal lead wires were soldered to the wires coming out of the Dewar proved to be critical. The small loops present there would pick up the "jitter" in the field of the magnet and would increase the noise in the signal drastically. It was necessary to minimize the magnetic pick-up by means of a driven coil placed under the crystal with the plane of the coil parallel to the planes of the large crystal faces. The signal from the crystal leads was fed into a lock-in amplifier and minimized by proper orientation of each of the three solder-joint loops. The minimizing process always produced minimum noise and was done prior to the performing of each experiment.

The crystal was fastened to a phenolic support table located at the bottom of the crystal holder assembly. Extreme care was taken to be sure the crystal had not changed its orientation during the course of the several experiments.

When the crystal finally had to be taken up, care was used to return the crystal to its original geometry.

It was necessary to determine the orientation of the crystal when inside the Dewar by some method accessible to the outside. For this purpose, two mirrors were cemented to the crystal holder. One of the mirrors was cemented to the phenolic end of the crystal holder near the crystal itself; care was taken to get this mirror as flat as possible on the phenolic base so that the normals to the crystal surface and the mirror would be parallel.

The second mirror was attached to the brass plate at the top of the holder and was oriented so that its normal and the normal to the mirror below defined a plane that was parallel to the axis of the crystal holder.

A larger mirror was cemented to the pole of the magnet so that its normal was parallel to the magnetic field. The crystal holder was then oriented in the Dewar so that the normals to the two mirrors on the holder and the normal to the mirror on the magnet were in the same vertical plane. Once this was accomplished, a scribe mark was made on the brass plate and mounting plate of the Dewar. This mark allowed the crystal holder to be returned to the same orientation each time it was returned to the Dewar. The crystal was oriented in this process so that its large face was perpendicular to the magnetic field. In this geometry, the

hexagonal axis was parallel to the direction of the magnetic field.

In addition to the mirror method of determining the orientation of the crystal while inside the Dewar, there was available a method independent of placement of mirrors. For cadmium, a minimum in the magnetoresistance occurs when the magnetic field is parallel to the hexagonal axis. This minimum is very sharp and clearly defined. Once the orientation of the crystal had been approximately determined with the mirror method, it was checked by means of locating the minimum of the magnetoresistance. Thus, all angles discussed in this article are taken with respect to the magnetoresistance minimum unless otherwise stated.

In order to test the effect of a zinc plating on the amplitude of the fundamental size-effect oscillation, it was decided to plate progressively thicker coatings of zinc onto the crystal while keeping all other parameters constant. The following plating solution (1) was prepared:

Zinc as metal	49.00 grams/liter
Total cyanide	142.00 grams/liter
Caustic soda	120.00 grams/liter
Sodium sulfide	0.75 grams/liter
Anode	99.9% pure strip zinc

This solution was found to be suitable over a wide range of temperatures centered around room temperature and acted acceptably under widely varying current densities.

Experience proved that the performance of the solution did not depend upon the orientation or location of the anode. A Heathkit power supply was used for the plating.

Zinc was deposited at the rate of 0.005617 microns per second at a current density of 11.85 milliamperes per square centimeter at the cathode. It was necessary to use such a low current density because higher current densities caused gas to be evolved at the cathode, causing pitting of the zinc. The thickness of the zinc coatings plated onto the crystal varied from one micron to ten microns.

The crystal was finally given a ten-micron coating of zinc on the back side where the leads were fastened and the front surface was given an electropolish. The electropolish (2) was performed in a solution of 250 milliliters of phosphoric acid and 250 milliliters of distilled water. A copper cathode was used because copper does not react with the polishing solution. A two-volt transistorized power supply was used to electropolish the cadmium.

To obtain current for experimental purposes, the current leads were attached to a twelve-volt car battery through a decade box, which was used to regulate the current. The current was monitored by means of a digital voltmeter reading across a one-ohm standard resistor that was connected in series with a current lead at the decade box.

To measure the resistance of the crystal, the voltage drop between any pair of potential probes was measured when

a constant known current was being passed through the crystal. The signal coming off the crystal was fed into a Keithley model 148 nanovoltmeter to be amplified and then introduced into a Honeywell model 2768 six-dial Rubicon microvolt potentiometer which had been internally wrapped with type AA Co-Netic metal foil to shield the instrument against stray magnetic fields. The offbalance voltage of the potentiometer was recorded on a Sargent model SRG strip-chart recorder.

Care was taken to shield the entire equipment from electric and magnetic fields, in addition to unfavorable thermal gradients. An inter-8 weave cable shielded with Co-Netic braid was employed to connect the galvanometer terminals to the input terminals of the Keithley nanovoltmeter. The current battery and the two batteries used with the potentiometer were placed in aluminum boxes. Only one earth ground was used in the entire system to avoid any possibility of forming a ground loop. The galvanometer terminals of the potentiometer were wrapped with several thick layers of cotton to minimize instrumental drift due to thermal effects.

The experiments were performed in a standard two-piece low temperature Dewar. When precooling with liquid nitrogen, care was taken to be sure the wall of the inner Dewar was flushed with air and pumped out, and the inner Dewar itself was filled with a helium gas atmosphere at a slight over-pressure. The Dewar was always precooled for at least two

hours to minimize the loss of liquid helium during transferring.

The experiments were performed at 1.312 degrees Kelvin by pumping on the helium with a Kinney high-capacity vacuum pump. The vapor pressure of the helium was measured with an oil manometer to determine the temperature of the helium bath. Care was taken in each experiment to be sure the level of the liquid helium remained above the entire crystal to prevent thermal effects.

Each time an experiment was performed the magnetoresistance was taken at room temperature and at 4.2 degrees Kelvin. The measurements were always taken with plus and minus currents so that the average value would average out any thermal effects still present.

In each experiment the Hall voltage was recorded as the magnetic field was swept from zero to five-thousand gauss. For each thickness of zinc plating on the crystal, the fundamental size-effect oscillations were recorded at zero degrees and minus four degrees as read on the inner-polar scale of the magnet. At each position a five-minute sweep and a twenty-five-minute sweep were taken. The five-minute sweep was taken using the one-microvolt-full-scale setting on the nanovoltmeter and the twenty-five-minute sweep was taken using the one-tenth-microvolt-full-scale setting on the nanovoltmeter. In addition, with a thickness of six microns zinc plating on the front surfaces of the crystal,

the fundamental size-effect oscillations were recorded from minus ten to plus ten degrees using five-minute sweeps and the one-microvolt-full-scale setting on the nanovoltmeter. Later, with nine microns of zinc plated onto the back of the crystal and the front surface of the crystal electropolished, this polar study was extended to plus and minus twenty degrees.

CHAPTER BIBLIOGRAPHY

1. Brimi, Marjorie A. and James R. Luck, Electrofinishing, New York, American Elsevier Publishing Company, Inc., 1965.

2. Fielder, James T., "Effect of Sample Geometry on Magnetomorphic Oscillations in the Hall Effect in Cadmium at Liquid Helium Temperatures," unpublished master's thesis, Department of Physics, North Texas State University, Denton, Texas, 1966.

CHAPTER III

THEORY

The size-effect oscillations in cadmium due to the lens-shaped pocket of electrons in the third Brillouin zone have been studied by Grenier, et al. (2), Zebouni, et al. (6), and Mackey, et al. (5, 6) with the magnetic field parallel to the hexagonal axis of the crystal.

Using the magnetoacoustic effect, Daniel and MacKinnon (1) have studied the geometry of the lens and mapped it. They have shown that the lens is a surface of revolution about the hexagonal axis and have given values for the dimensions of the lens and the lattice spacings. Assuming that cadmium had two conduction electrons per atom and using their values for the lattice spacings, they calculated the Fermi sphere that would just accommodate these electrons as free electrons to have a radius of 1.410 inverse angstroms. The Fermi sphere of cadmium is shown with respect to the Brillouin zone boundaries in Figure 1 (see Appendix for all figures). The construction suggested by Harrison (1) leads to the Fermi surface as shown in Figure 2. The lens closely approximates the free-electron surface but is rounded at the edges such that the surface contacts the zone boundary at a 90° angle.

Gurevich (3) has shown that the period of the size-effect oscillations is proportional to the Gaussian radius of curvature at any elliptic point where the normal to the Fermi surface is parallel to the magnetic field. Figure 3 shows the geometry of this situation. Theta is the angle between the normal to the large face of the crystal and the direction of the field. Due to the special geometry used in the present experiments, theta is the angle between the hexagonal axis and the direction of the field.

Gurevich obtained an equation relating the Gaussian radius of curvature of the Fermi surface to the period of the oscillations and the angle between the magnetic field and the crystal normal. He found that

(1) $$g(\theta) = \frac{P_0(\theta)\ ea}{hc\ \cos\ \theta}$$

where

h is Planck's constant

P_0 is the period of the size-effect oscillations expressed in Gauss.

e is the electronic charge expressed in esu units.

c is the speed of light expressed in cgs units.

a is the crystal thickness in centimeters.

θ is the angle between the crystal normal and the direction of the magnetic field.

$g(\theta)$ is the Gaussian radius of curvature in $\vec{k}$-space at the elliptic point where the Fermi surface normal is parallel to the magnetic field.

To understand this equation more fully, consider what is meant by "Gaussian curvature of a surface at an elliptic point." Consider a general surface S as in Figure 4, where P is an elliptic point of S (i.e., lies entirely on one side of the tangent plane in the neighborhood of P).

The vector $\vec{n}$ is a unit vector normal to the surface and Q is a plane that contains the normal vector. The intersection of Q with S forms a space curve, AB. The curvature of AB at P is $\vec{K} = \frac{d\vec{t}}{dS}$, where t is a unit vector tangent to curve AB and dS is an element of length measured along AB in the direction of $\vec{t}$. $\vec{K}\cdot\vec{n}$ is the normal curvature of S at the point P. The radius of normal curvature is $R_n = 1/(\vec{K}\cdot\vec{n})$.

When the plane making the normal section turns around the normal line of S at P, the normal section varies and the normal curvature varies, attaining some maximum and some minimum value. The extreme values are called the principal normal curvatures at the point P of the surface S.

It can be shown (4) that there is just one direction for which the normal curvature is a maximum and just one direction for which it is a minimum. These directions of principal curvature can be shown to be orthogonal. The associated radii of normal curvature are a minimum and a maximum.

It can be shown that (4) for the case of a surface of revolution about the z axis, whose profile is z = f(u) as in

Figure 5, the principal normal radii of curvature at a point of the surface of revolution are given by the formulas:

$$(2)\quad \frac{1}{R_1} = f''/(1 + f'^2)^{3/2}, \quad \frac{1}{R_2} = f'/u(1 + f'^2)^{1/2}.$$

The radius R_1 is equal in length to the radius of curvature of a meridian, while the radius R_2 is equal in length to the segment of the normal line between the surface and the axis of revolution.

For the experiment under consideration here, the function f(u) is the equation of the Fermi surface in the third Brillouin zone and the variable u is to be defined later in terms of the k-vector in the third Brillouin zone.

The Gaussian curvature $g(\theta)$ at a point P of a surface S is the square root of the product of the principal normal radii of curvature of S at P. Thus, one finds that

$$(3)\qquad g(\theta) = \sqrt{R_1 R_2}.$$

The Fermi surface of cadmium is shown with respect to the Brillouin zone boundaries in Figures 6 and 7. Figure 8 shows the Fermi surface in the third Brillouin zone of cadmium.

Ziman (7) has developed an equation for the Fermi surface in the neighborhood of a Brillouin zone:

$$(4)\quad \mathcal{E}(\vec{G} + \vec{K}) = \left[\frac{1}{2}\mathcal{E}_{G-} + \mathcal{E}_{G+}\right] + \frac{\hbar^2 k^2}{2m} + \frac{1}{2}\left\{\left(\mathcal{E}_{G+} - \mathcal{E}_{G-}\right)^2 + 16\left(\frac{\hbar^2}{2m}\vec{G}\cdot\vec{k}\right)^2\right\}^{Y_2}$$

where

$\mathcal{E}_{G-}$ is the energy associated with the zone boundary, approaching the boundary in the direction of increasing k.

$\mathcal{E}_{G+}$ is the energy associated with the zone boundary, approaching the boundary in the direction of decreasing k.

$\vec{G}$ is the reciprocal lattice vector from the center of the first Brillouin zone to the boundary in question.

$\mathcal{E}(\vec{G} + \vec{k})$ is the electron energy with respect to the center of the first Brillouin zone.

Notice that

$$\frac{1}{2}\left(\mathcal{E}_{G-} + \mathcal{E}_{G+}\right) = \mathcal{E}_{G+} - \frac{1}{2}\Delta\mathcal{E} \tag{5}$$

since

$$\Delta = {}_{G+} - {}_{G-}.$$

Using the above, equation (4) becomes

$$\mathcal{E}(\vec{G} + \vec{k}) = \mathcal{E}_{G+} - \frac{\Delta\mathcal{E}}{2} + \frac{\hbar^2 k^2}{2m} + \left\{\frac{1}{2}(\Delta\mathcal{E})^2 + 16\left[\frac{\hbar^2}{2m}(\vec{G}\cdot\vec{k})\right]^2\right\}^{y_2}. \tag{6}$$

It is desired to obtain the equation of the Fermi surface of cadmium in the third Brillouin zone using the Ziman equation. To do this, the energy to the center of the energy band discontinuity at the boundary between the second and third zone, the energy gap, and the energy of the Fermi

surface relative to the boundary of the third Brillouin zone are required. Thus,

$$\mathcal{E}(\vec{G} + \vec{k}) = \mathcal{E}(\vec{G}) + \frac{1}{2}\Delta\mathcal{E} + \mathcal{E}(\vec{k}). \tag{7}$$

The energy of the Fermi surface relative to the third zone boundary is

$$\mathcal{E}(\vec{K}) = \mathcal{E}_f = \left(\frac{\hbar^2}{2m}\right)|\vec{K}|^2 \tag{8}$$

where $k_z = 0$ and $\vec{K}$ lies on the edge of the lens.

Using the value of $|\vec{K}| = 0.725$ for the edge of the lens (1) this becomes

$$\mathcal{E}_f = (3.806)(0.725)^2 = 2.000 \text{ e.v.}, \tag{9}$$

where e.806 is a conversion factor used to make the value of $\mathcal{E}_f$ appear as electron volts when k is given in inverse angstroms.

Now the energy of the gap between the second and third zones can be calculated using

$$\mathcal{E}_f = -\left(\frac{1}{2}\right)\Delta\mathcal{E} + \left(\frac{\hbar^2}{2m}\right)k^2 + \frac{1}{2}\left\{(\Delta\mathcal{E})^2 + 16\left[\frac{\hbar^2}{2m}(\vec{G}\cdot\vec{k})\right]^2\right\}^{y_2}. \tag{10}$$

Solving the above equation for Δ , one finds that

$$\Delta\mathcal{E} = \frac{b - a^2}{2a} \tag{11}$$

where

$$a = 2\mathcal{E}_f - \left(\frac{\hbar^2}{m}\right)k^2 \tag{12}$$

(13) $$b = 16\left[\frac{\hbar^2}{2m}\,(\vec{G}\cdot\vec{k})\right]^2.$$

Using the values of $k_1 = k_2 = 0$, and $k_3 = 0.250$ as quoted by Daniel and MacKinnon for the apex of the lens, one finds that

(14) $$a = 3.5242 \text{ e.v.}$$

(15) $$b = 18.6936 \text{ (e.v.)}^2$$

With the values of a and b known, $\Delta\mathcal{E}$ becomes 0.8901 electron volts.

Using the value $|\vec{G}| = 1.136\ \mathring{A}^{-1} = \frac{2\pi}{c}$, where c is the lattice spacing in the direction of the hexagonal axis, one finds that

(16) $$\mathcal{E}(\vec{G}) = \frac{\hbar^2}{2m}\,G^2 = (3.806)(1.136)^2 = 4.916 \text{ e.v.}$$

Thus we obtain the Fermi energy measured relative to the center of the first zone to be $\mathcal{E}(\vec{G} + \vec{k}) = 7.3566$ electron volts.

With the above calculated constants, the equation of the Fermi surface is found from equation (6) to be

(17) $$4.8901 = 7.6120(k_1^2 + k_2^2 + k_3^2) + \{0.7922 + (299.1000)k_3^2\}^{y_2}.$$

This may be written as

(18) $$4.8901 = 7.6120(u^2 + k_3^2) + \{0.7922 + (299.1000)k_3^2\}^{y_2}.$$

Equation (18) was solved for u. Once this was done, k_3 was divided into 100 increments between its minimum value of zero and its maximum value of 0.250 inverse angstroms. Then

equation (18) was solved for u for each of the 100 values of k_3. With the values of u and k_3 known, the Gaussian radius of curvature was calculated at each coordinate point, (u_i, k_{3i}). The values so obtained were compared with experimentally observed values.

CHAPTER BIBLIOGRAPHY

1. Daniel, M. R. and L. MacKinnon, "The Magnetoacoustic Effect and the Fermi Surface of Cadmium," Philosophical Magazine, VIII (April, 1963), 537-552.

2. Grenier, C. G., K. R. Efferson, and J. M. Reynolds, "Magnetic Field Dependence of the Size Effect in the Transport Coefficients of a Cadmium Single Crystal at Liquid Helium Temperatures," Physical Review, CXLIII (March, 1966), 406-420.

3. Gurevich, V. L., "Oscillations in the Conductivity of Metallic Films in Magnetic Fields," Soviet Physics JETP 8 (March, 1959), 464-470.

4. Lane, E. P., Metric Differential Geometry of Curves and Surfaces, Chicago, The University of Chicago Press, 1940.

5. Mackey, H. J., J. R. Sybert, and J. T. Fielder, "Effect of Sample Geometry on Magnetomorphic Oscillations in the Hall Effect in Cadmium at Liquid-Helium Temperatures," Physical Review, CLVII (May, 1967), 578-585.

6. Zebouni, N. H., R. E. Hamburg, and H. J. Mackey, "Magnetomorphic Oscillations in the Hall Effect and Magnetoresistance in Cadmium," Physical Review Letters, XI (September, 1963), 260-264.

7. Ziman, J. M., Electrons and Phonons, London, Oxford University Press, 1960.

CHAPTER IV

ANALYSIS AND CONCLUSIONS

Effect of the Zinc Plating

The addition of successive thicknesses of zinc on the upper six-cut face of the crystal appeared to increase drastically the amplitude of the oscillation which was recorded on the strip chart. The fact that the amplitude was apparently increased was interpreted to mean that the scattering at the plated surface was significantly more diffuse than the scattering at the six-cut surface. Therefore the set of experiments was performed again using a larger range of zinc thicknesses. The effect appeared to saturate for a zinc layer as large as nine microns.

The voltage data from the strip chart records were processed on an IBM 1620 to obtain curves of Hall resistivity, ρ_{21} versus H. A third order polynomial was fitted to each curve by the method of least squares, and the difference between the exponential ρ_{21} and the fitted curve gave the oscillatory component $\tilde{\rho}_{21}$ versus H, as indicated in Figure 9. These oscillatory curves for each zinc thickness were plotted and examined. At this point it was discovered that the amplitude of $\tilde{\rho}_{21}$ was in fact independent of the zinc treatment. Examination of the various cubics representative of the gross

effect showed that the amplitude of the gross ρ_{21} was diminished so that the amplitude of the superimposed $\tilde{\rho}_{21}$ only appeared to be enhanced. Thus the nature of the electron scattering appears to be independent of the presence of a zinc over-layer, implying that the scattering was already essentially diffuse at the six-cut surfaces.

The period of the oscillations in each sample was determined by plotting the field positions of maxima and minima against successive integers and half-integers. A least-squares straight line was fitted through these data as shown in Figure 10 and the slope of the lines gave the periods directly. No variation in period was found for the samples with zinc coatings, which was to be expected in that the maximum variation in sample thickness was only 1.2 per cent, which is smaller than the accuracy of the period measurements.

The crystal was then electropolished on one surface, leaving a nine-micron zinc layer on the opposite face such that the sample thickness was reduced to 0.0662 centimeters exclusive of the zinc coating thickness. The oscillation $\tilde{\rho}_{21}$ was obtained as described previously The period was increased precisely by the inverse ratio of the two sample thicknesses.

If the scattering at the electropolished surface were more specular than at the coated surface it might be possible to observe harmonic content in the $\tilde{\rho}_{21}$. There was no

evidence of harmonic content found under the above conditions. Thus, the total effect of the zinc plating was only to modify the gross ρ_{21} and no evidence for modification of the surface scattering parameter was found.

Angular Dependence of the Amplitude

The oscillation $\tilde{\rho}_{21}$ was studied with regard to period and amplitude as the angle between the normal to the sample surface [0001] and the magnetic field was varied. Figure 11 shows the amplitude as a function of θ. The actual peak-to-peak voltage which appeared on the strip chart was only about fifty nanovolts for the largest amplitude which was observed at approximately eight degrees. The oscillations became obscured by noise when θ was increased to twenty degrees. Figure 12 illustrates the decrease in amplitude as the angle between the crystal normal and the magnetic field increases. Theoretically one may expect the following approximate relationship for the amplitude $|\tilde{\rho}_{21}|$ as a function of θ:

$$|\tilde{\rho}_{21}| \approx K(\theta)\ \alpha(\theta)\ \cos\ \theta, \tag{19}$$

where

$$\rho_{11} = [\alpha(\theta)\ H^2]^2 \tag{20}$$

and

$$|\tilde{\sigma}_{12}| = \frac{K(\theta)\ \cos\ \theta}{H^4} \tag{21}$$

Equation (20) expresses the fact that the magnetoresistivity of cadmium, ρ_{11}, is quadratic in H with the

coefficient α dependent on θ. The approximate variation of $\alpha(\theta)$ in relative units with θ may be inferred from Figure 13. Equation (21) represents the results of Gurevich's theory which indicates the amplitude of the oscillation in σ_{12} as a function of H and θ. The factor $K(\theta)$ depends on the differential geometry of the Fermi surface at the elliptic point where the normal is parallel to H. The factor $K(\theta)$ may be shown to be a decreasing function of θ, symmetric about the hexagonal direction. Equation (19) follows as the result of a tensor inversion, $\hat{\rho} = \hat{\sigma}^{-1}$, with $\rho_{11} >> \rho_{21}$. Note $K(\theta) \cos \theta$ is a decreasing function of θ while $\alpha(\theta)$ is, in the neighborhood of θ equal to zero, an increasing function of θ. $|\tilde{\rho}_{21}|$ results from the competition between these two factors.

Note that all factors should be symmetric about [0001]. However, close examination of Figure 13 shows that $\alpha(\theta)$ is somewhat skewed and not symmetric about θ equal to zero. This fact implies that the crystal may have been slightly cocked so that the symmetry axes of the crystal were not precisely parallel and perpendicular to the plane defined by the magnetic field as θ is varied.

From equation (19), one has

$$K(\theta) = \frac{|\tilde{\rho}_{21}|}{\alpha(\theta) \cos \theta} .$$

Figure 14 is a plot in relative units of the right hand member of equation (4) against θ. Note that the experimentally

determined $K(\theta)$ is approximately symmetric about θ equal to four degrees which is the position of the [0001] direction as determined by the mirror method. Clearly one needs to have a goniometer-type crystal holder so that the hexagonal axis may be located accurately by a study of the symmetry of ρ_{11} vs θ. Under these conditions one may be able to determine $K(\theta)$ with sufficient accuracy to compare with theory.

Angular Dependence of Period

The Gaussian radius of curvature, $g(\theta)$, at the elliptic point where the Fermi surface normal (i.e., the Fermi velocity) is parallel to the magnetic field determines the period of the oscillation $\tilde{\rho}_{21}$. Figure 15 shows $g(\theta)$, as computed from the Ziman equation, plotted against u for values in the range u = 0 to u = 0.725 corresponding to points on the lens ranging from the apex in the [0001] direction to the edge of the lens. The quantity $g(\theta)$ is seen to vary from a maximum of 1.36 $\mathring{A}^{-1}$ at u equal to 0 to a minimum of 0.152 $\mathring{A}^{-1}$ at u equal to 0.725 $\mathring{A}^{-1}$.

For a sample cut as in these experiments with [0001] normal to the crystal's large faces, the period should vary from a maximum for θ equal to zero, to zero at θ equal to $\frac{\pi}{2}$. The quantity $g(\theta)$ may be determined experimentally from

$$g(\theta) = \frac{e\ a\ P_0(\theta)}{h\ c\ \cos\ \theta} \cdot \tag{23}$$

These computed values may be compared to those exhibited in

Figure 15. It is more convenient to present the theoretical curve as shown in Figure 16; here $g(\theta)$ is plotted against θ directly.

Figure 17 shows the same curve as that of Figure 16 for $-12\ 1/2° \leq \theta \leq 16°$ along with the values of $g(\theta)$ as computed from equation (23) and the measured periods. Data from two separate runs appear on the graph and are appropriately labeled to distinguish one run from another.

Restriction to this narrow range of θ was necessary since the accuracy of the period measurements decreases rapidly as $|\theta|$ increases and the amplitude of $\tilde{\rho}_{21}$ decreases. It is clear that the experimental resolution is not high enough to verify the theoretical variation in $g(\theta)$. One should note, however, that the level of the voltages actually measured is in the 100 nanovolt realm, with the oscillation only a small fraction of this voltage. Agreement to the degree exhibited in Figure 17 is quite good from a percentage point of view.

Repetition of these experiments with more accurate experimental resolution should be rewarding. It is suggested that the use of an accurately calibrated Hall probe for close monitoring of the magnetic field would be particularly desirable. The use of an automatic, rapid data-taking device such as the magnetic tape unit now being devised should allow one to process feasibly fifty times as many data points per strip-chart record, and through computer

techniques one should be able to obtain the resolution that this study has demonstrated to be necessary in order to determine $g(\theta)$ accurately.

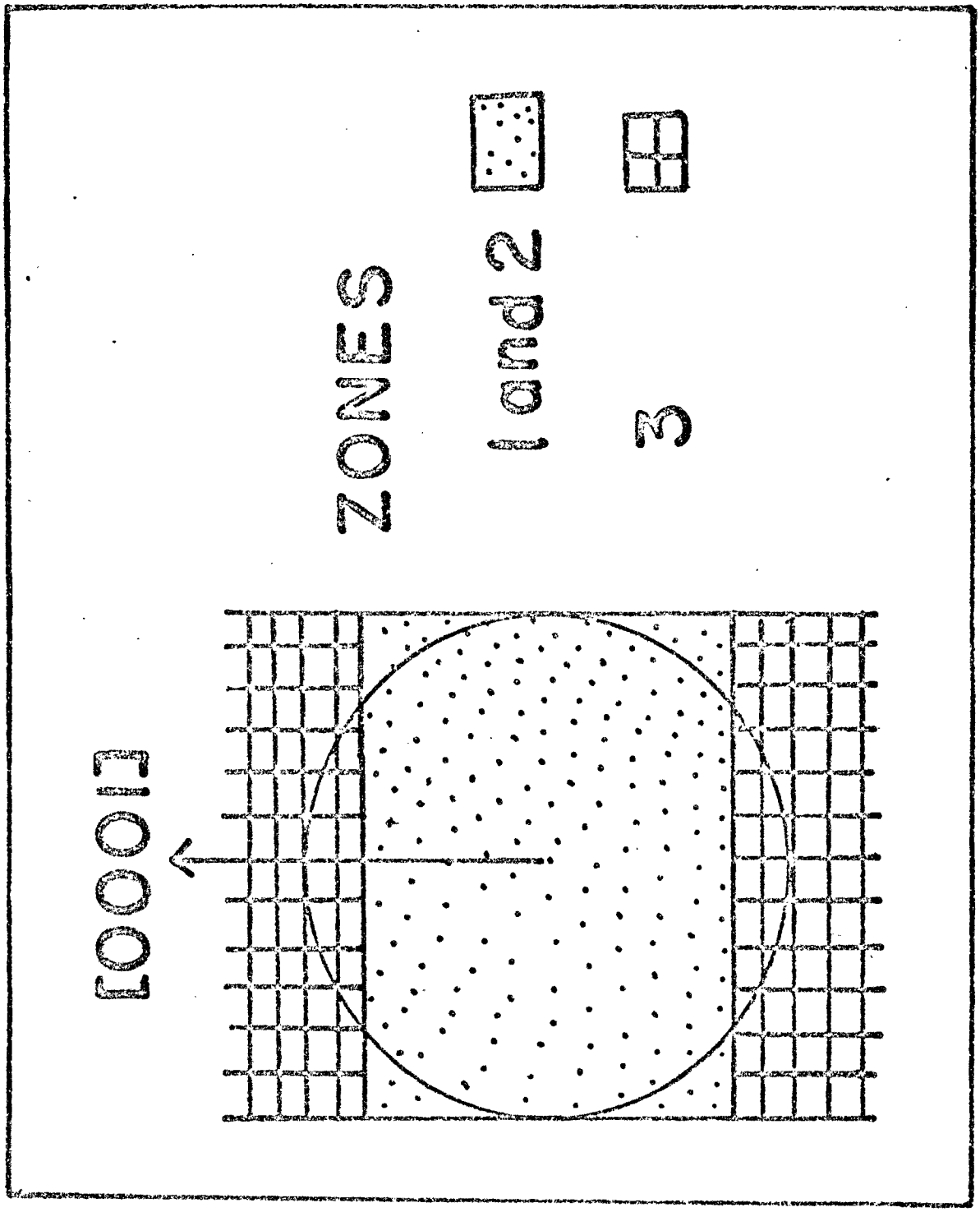

Fig. 1--Fermi surface of cadmium with respect to the Brillouin zones

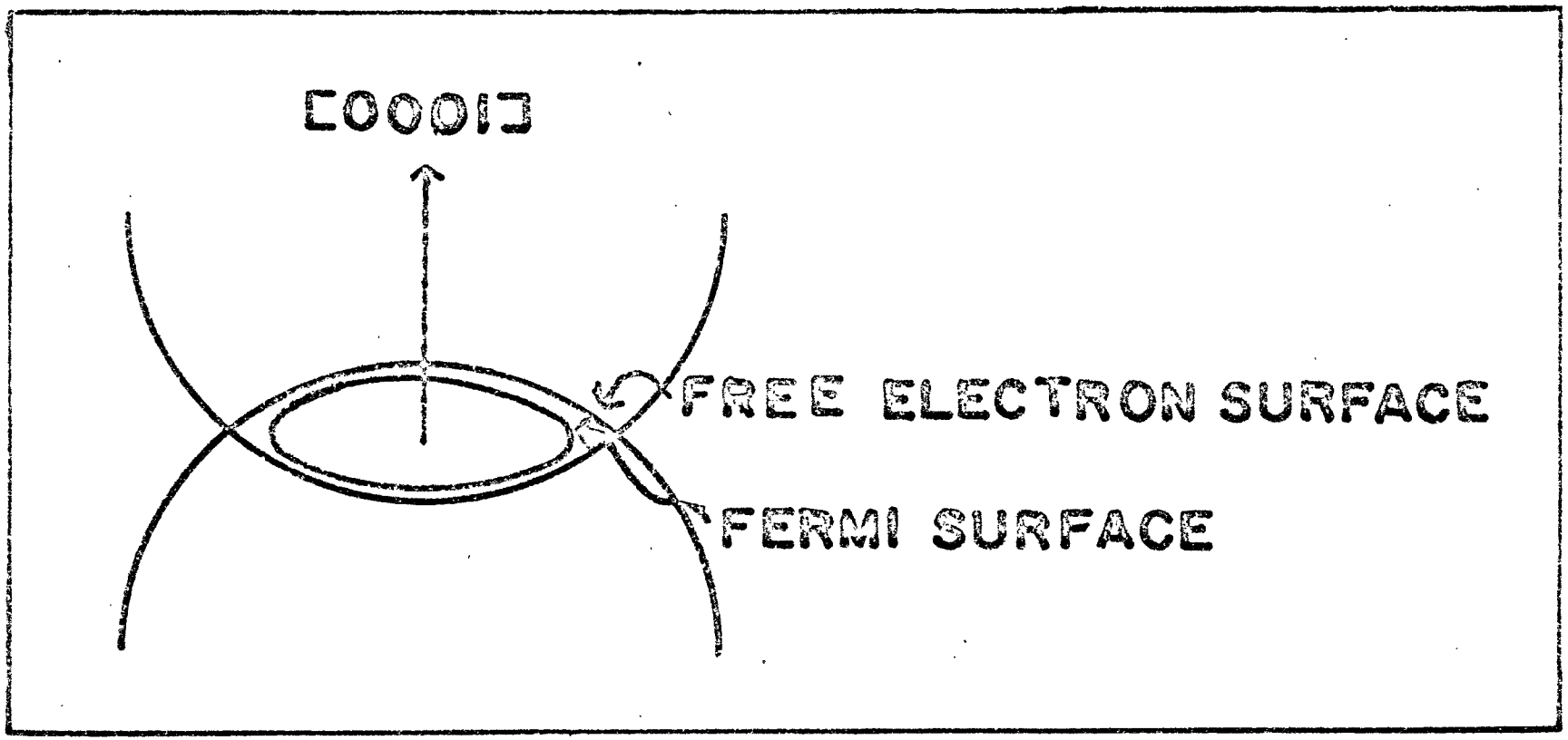

Fig. 2--Harrison's construction for Fermi surface in third Brillouin zone

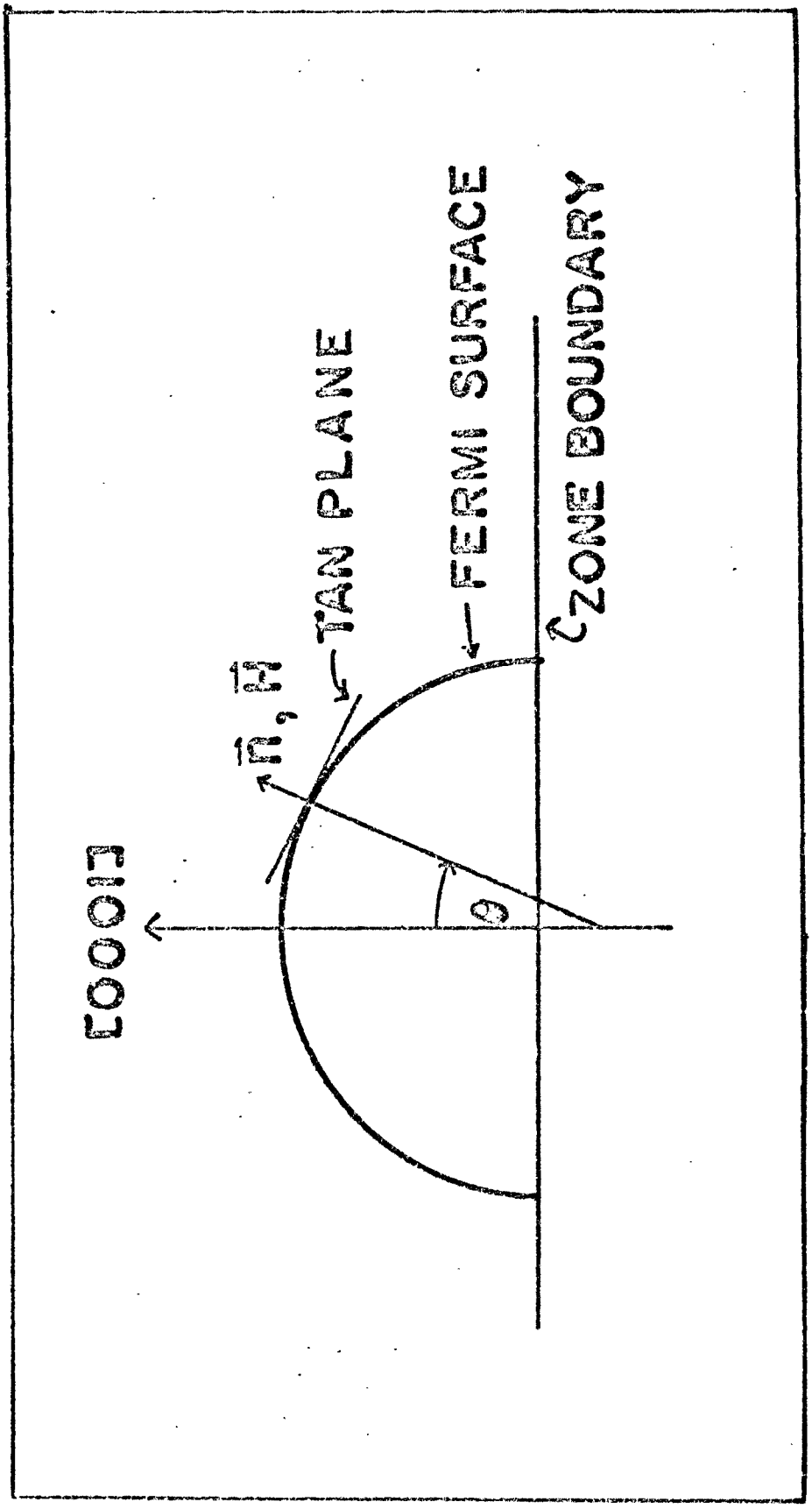

Fig. 3--Relation of Fermi surface to magnetic field

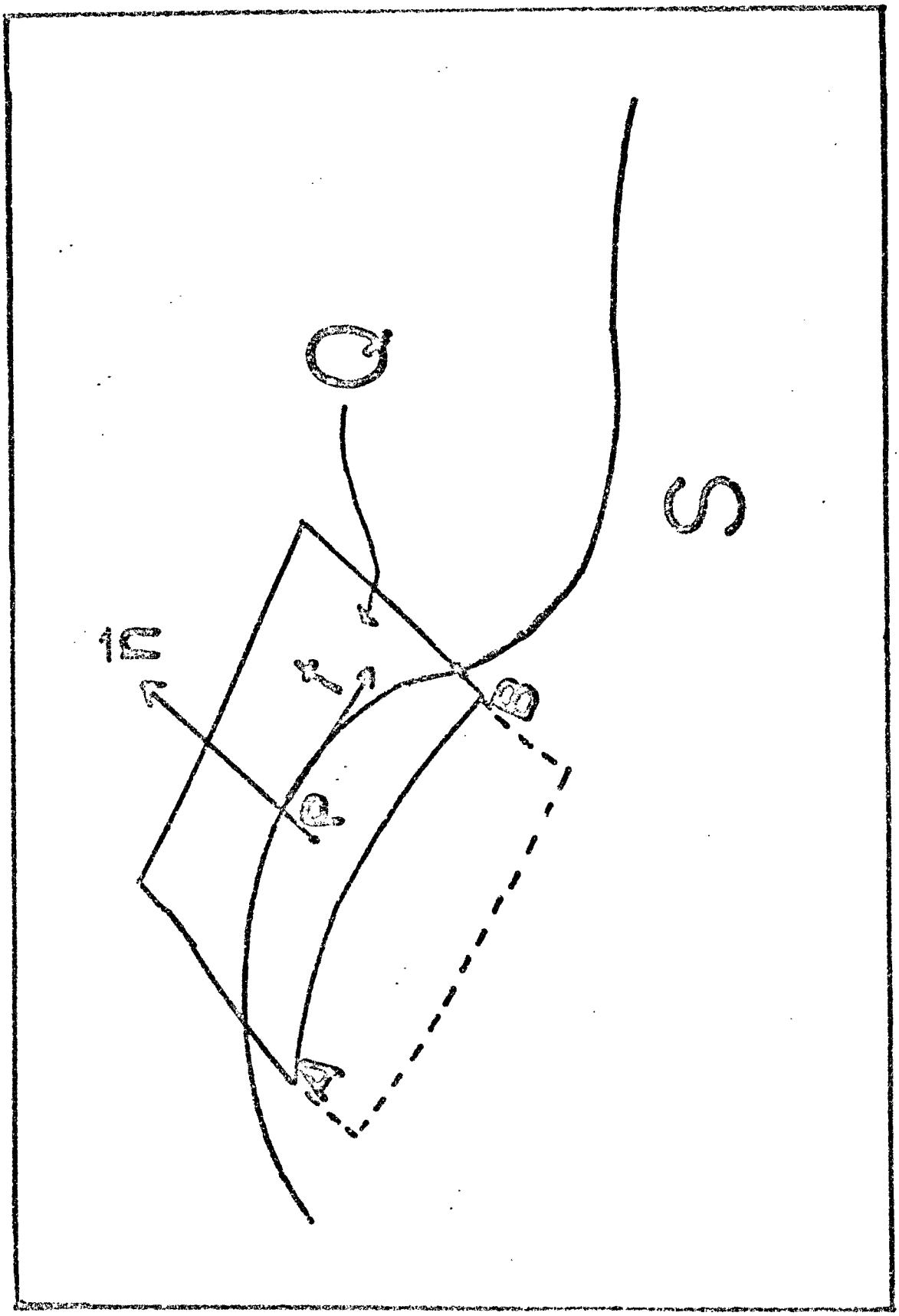

Fig. 4--Relation of the normal sections to the general surface

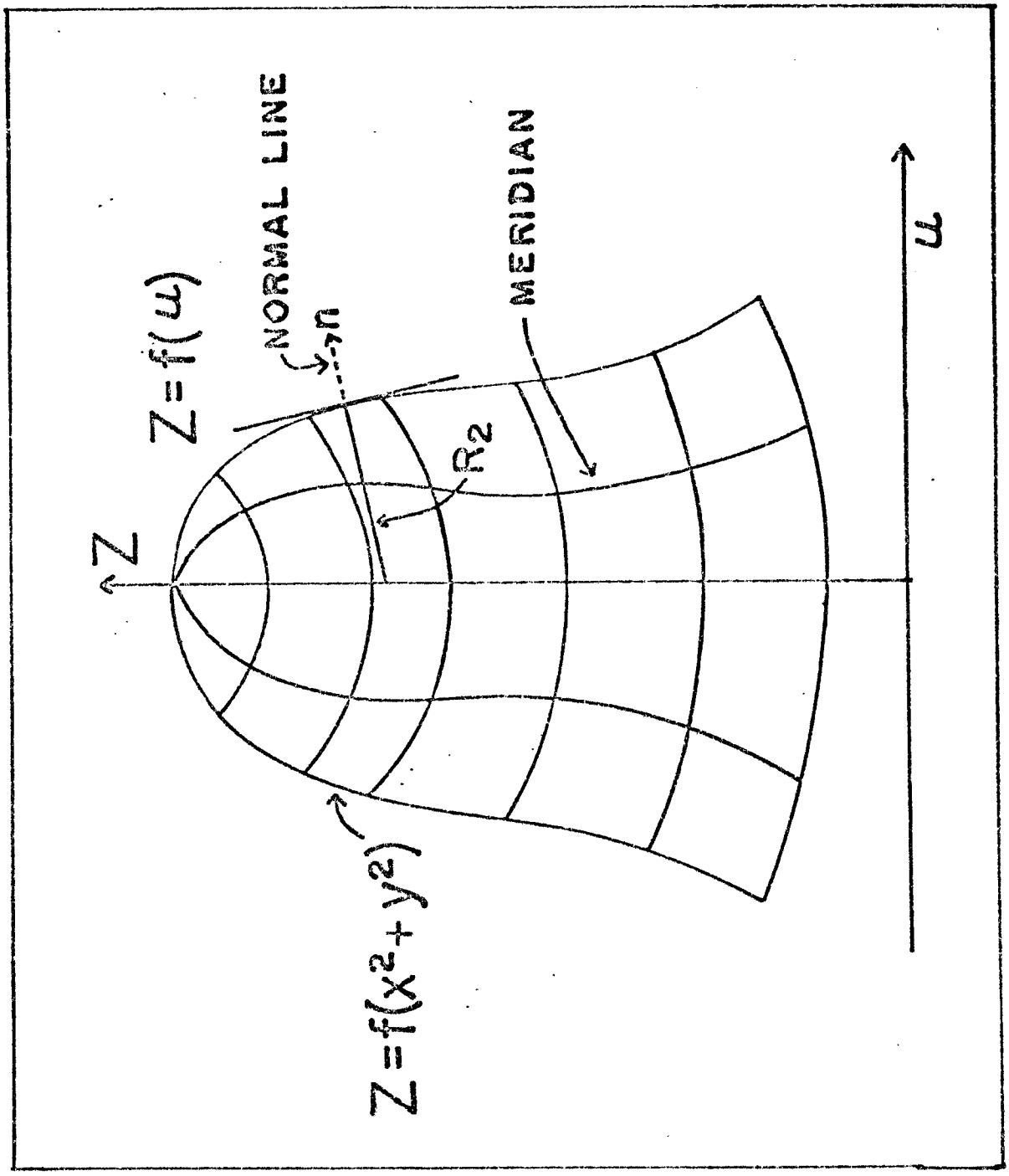

Fig. 5--A general surface of revolution about the Z-axis

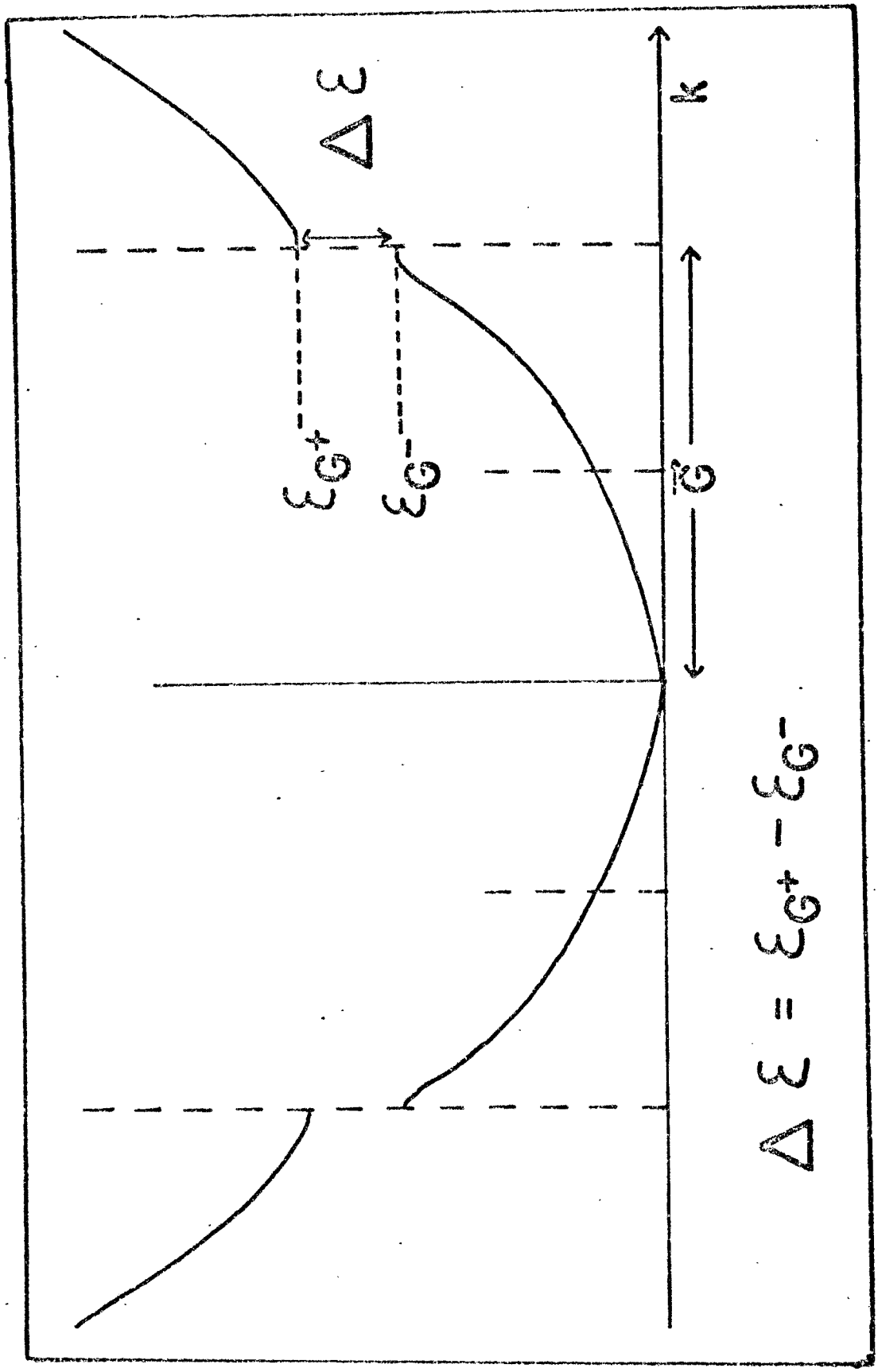

Fig. 6--Electron energy with respect to Brillouin zone boundaries

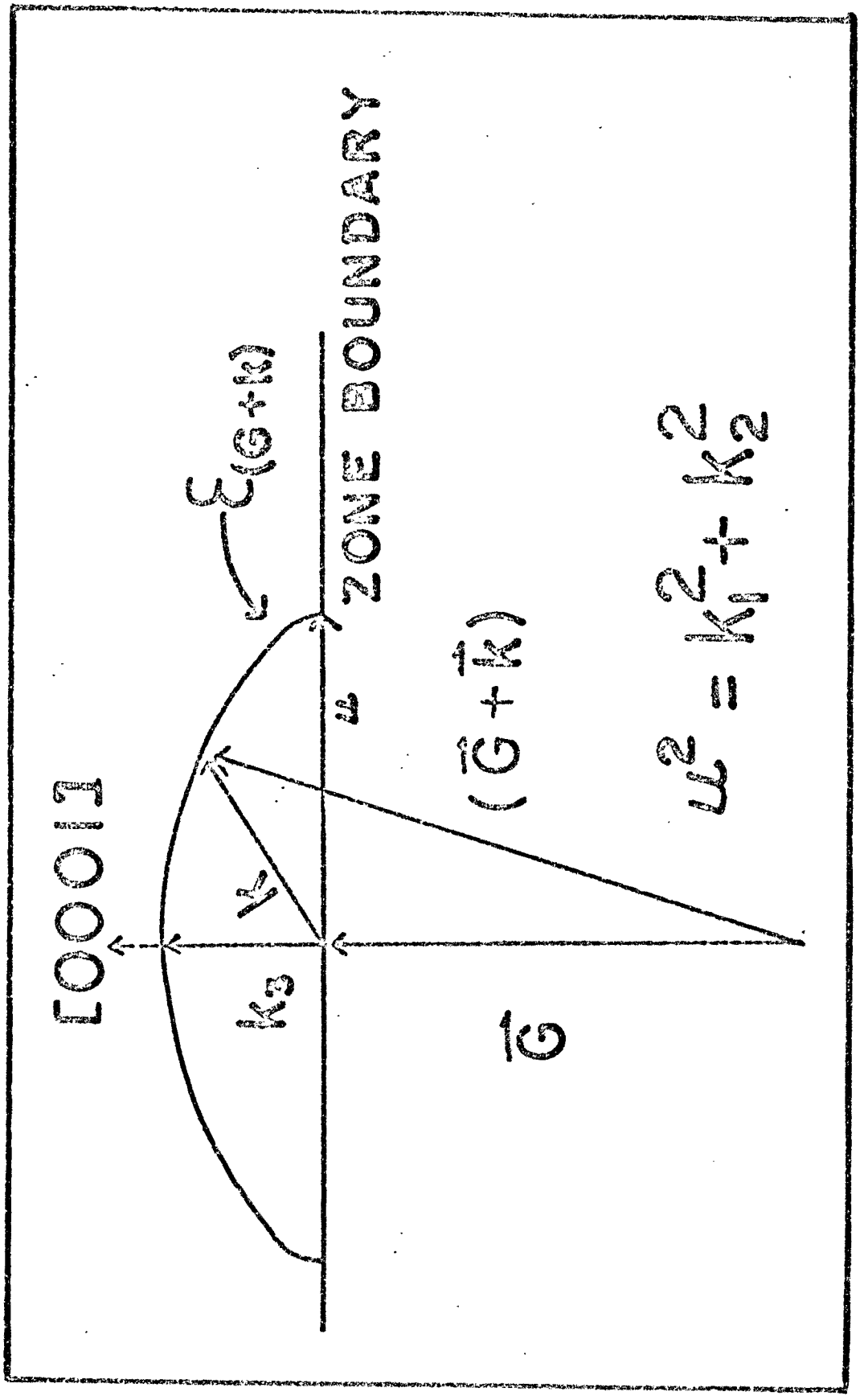

Fig. 7--Fermi surface of cadmium with respect to the boundary of the third Brillouin zone.

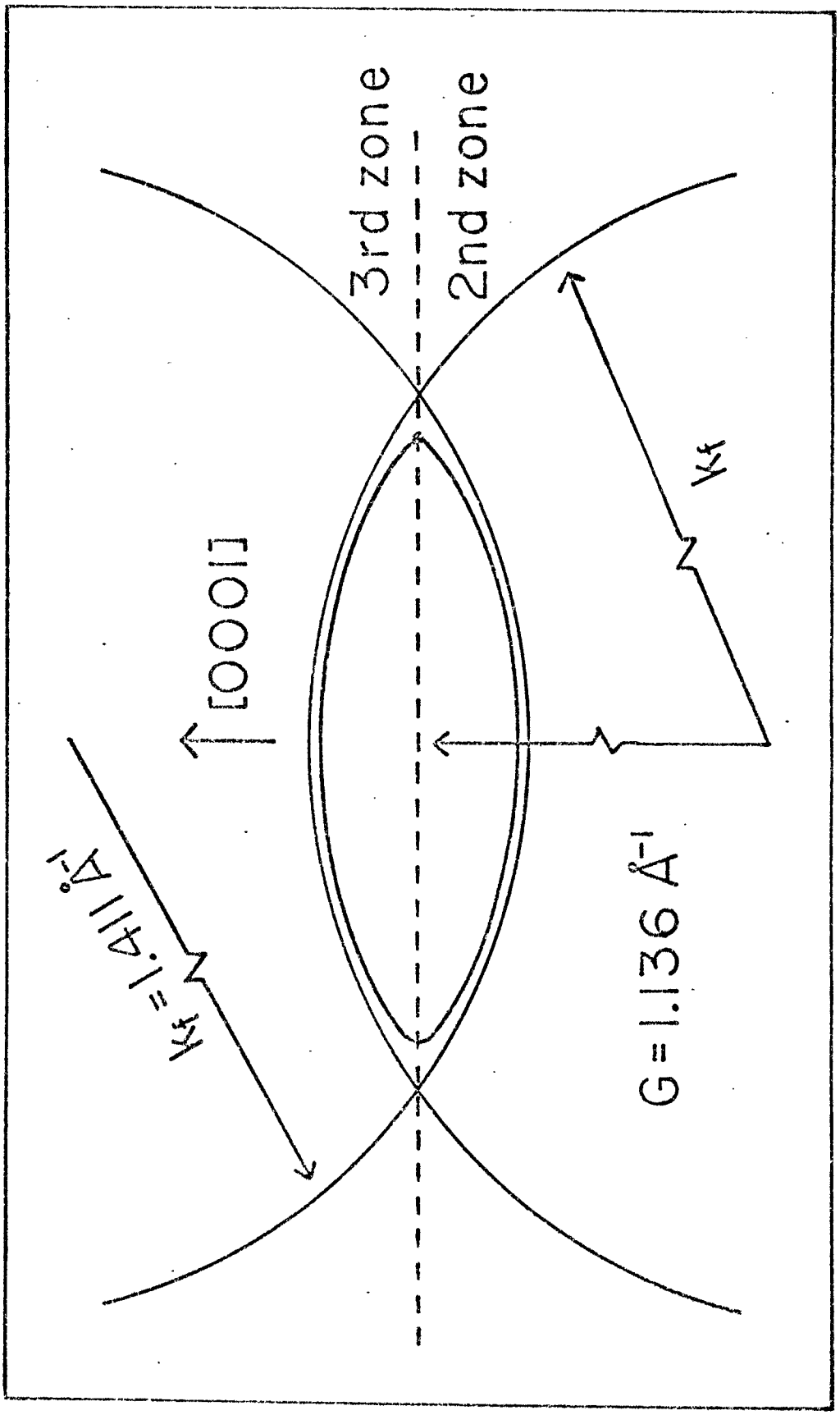

Fig. 8--Fermi surface of cadmium with respect to free electrons Fermi spheres

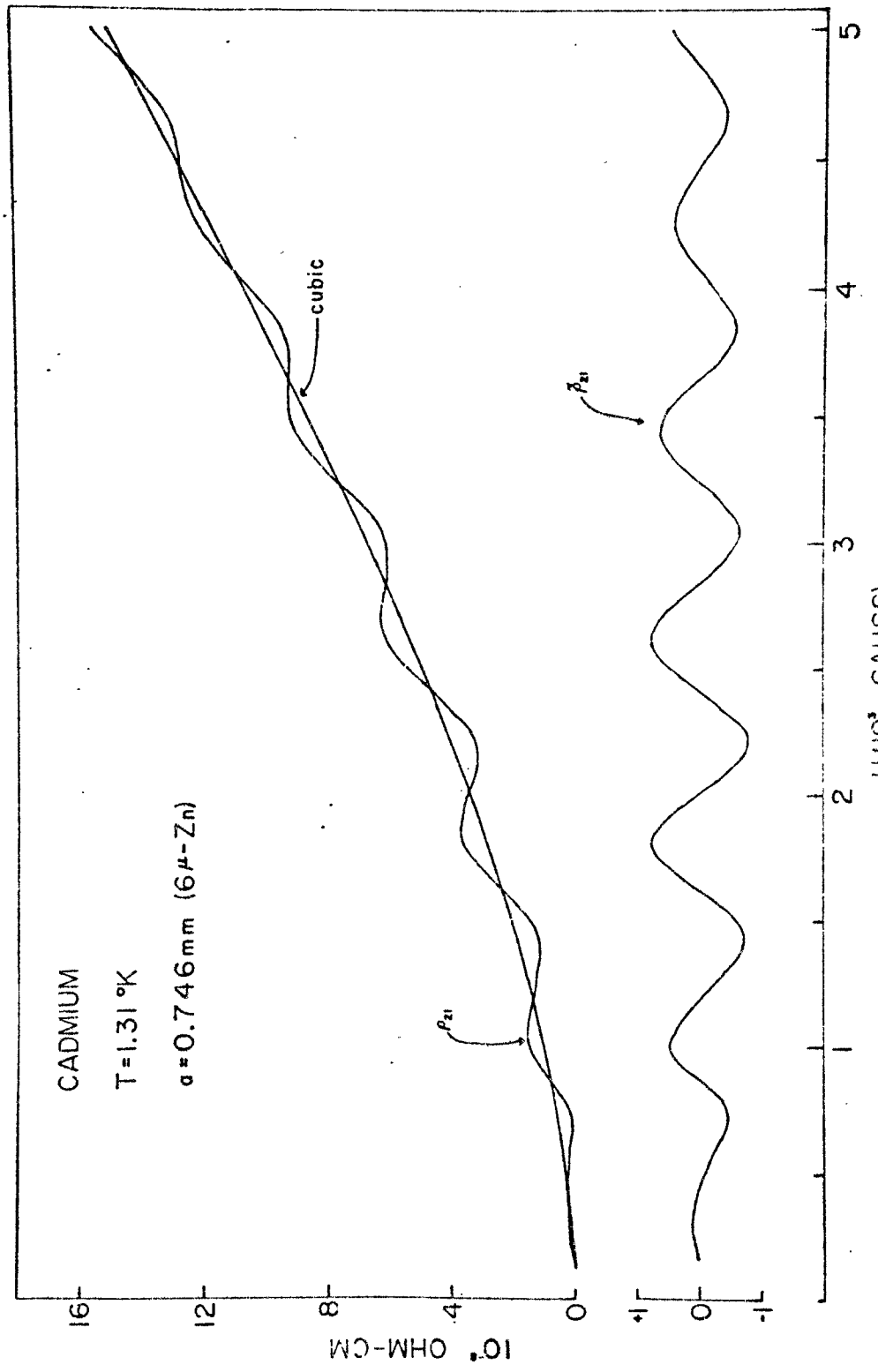

Fig. 9--Third order polynomial fit to gross ρ_{21}, showing oscillatory component.

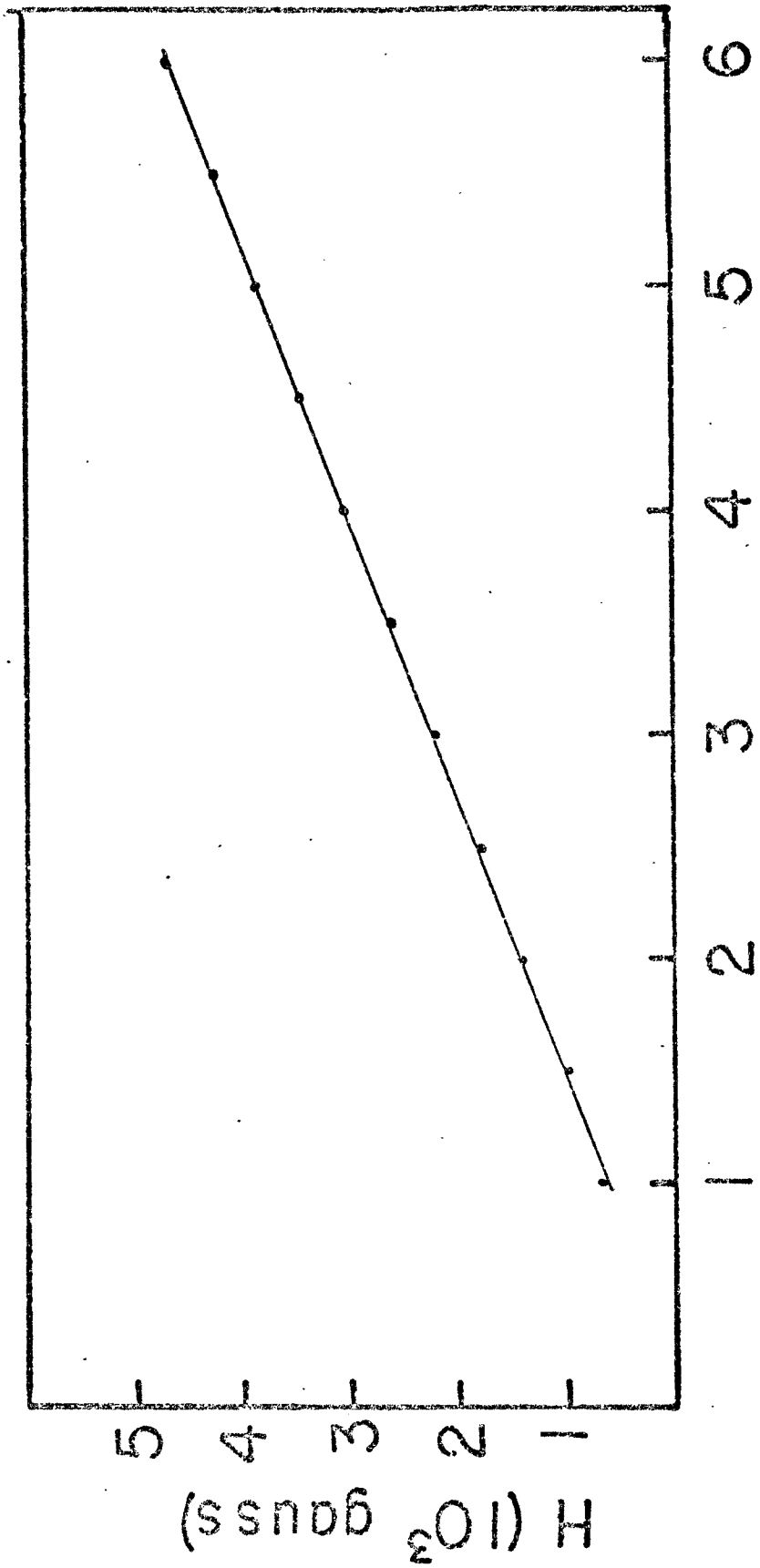

Fig. 10--Maximum and minimum field values of $\tilde{\rho}_{21}$ vs. integers

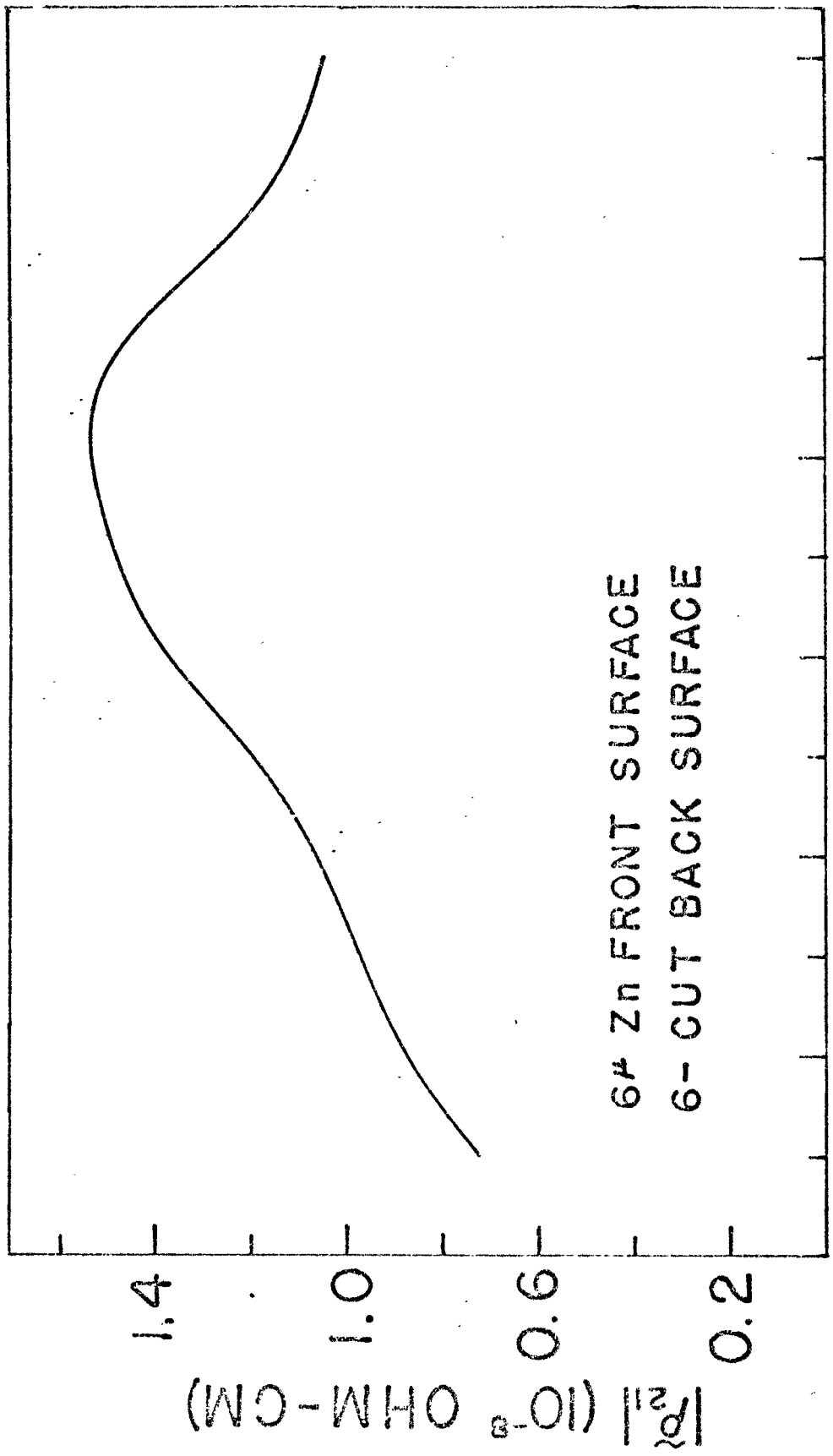

Fig. 11--Amplitude of $\tilde{\rho}_{21}$ vs. angle from hexagonal axis

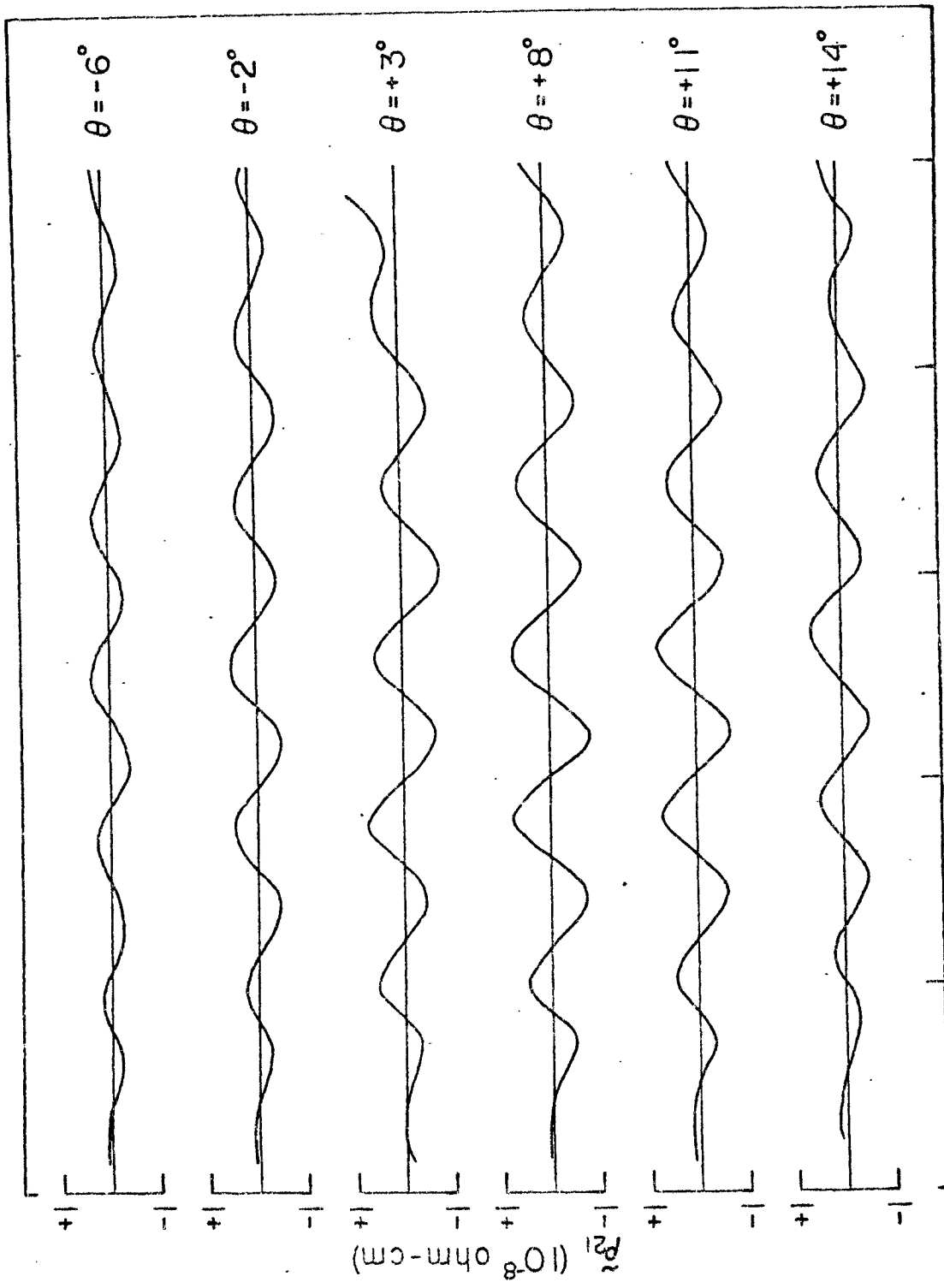

Fig. 12--Amplitude of $\tilde{\rho}_{21}$ as a function of the magnetic field and angle from hexagonal axis.

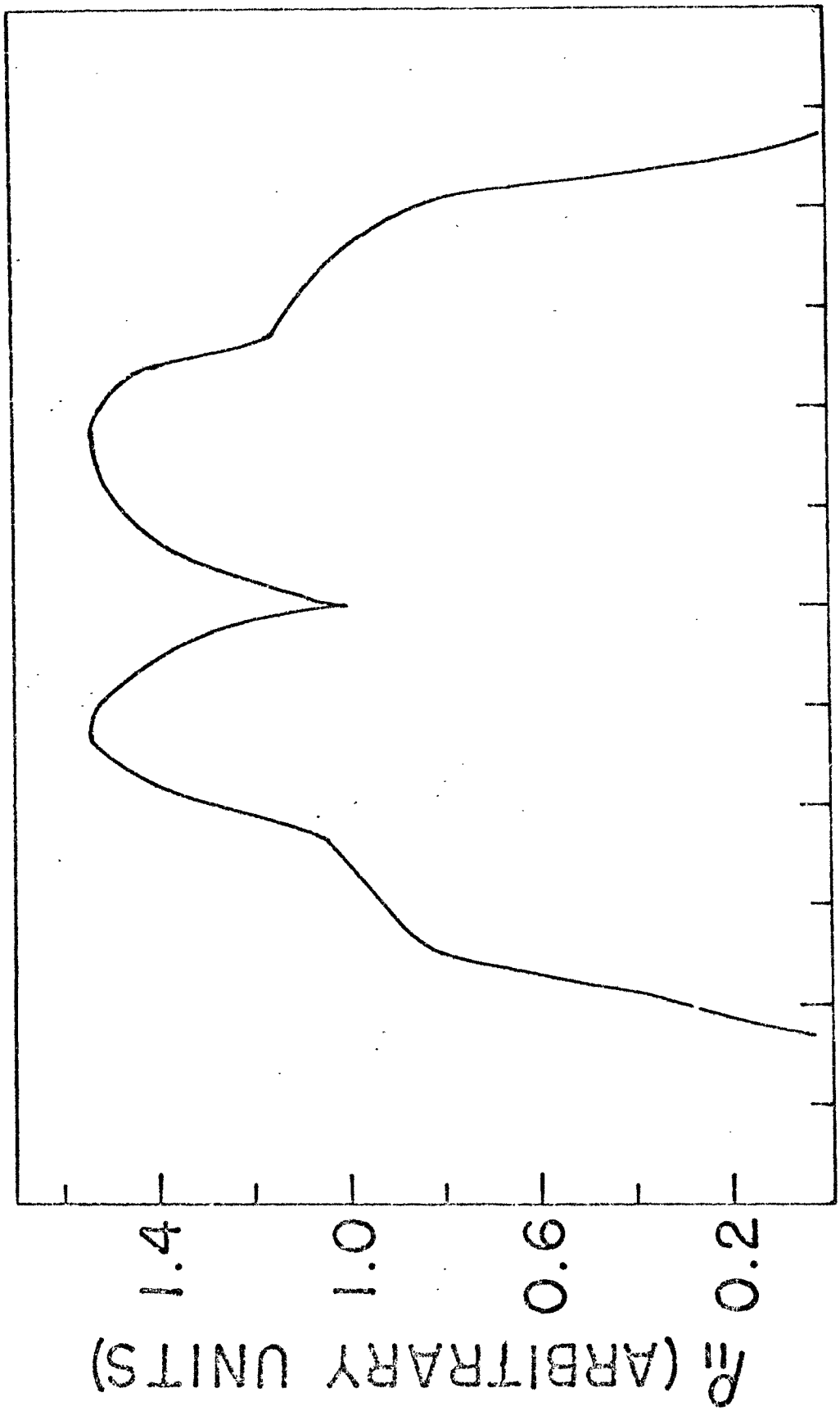

Fig. 13--ρ_{11} relative vs. angle from hexagonal axis

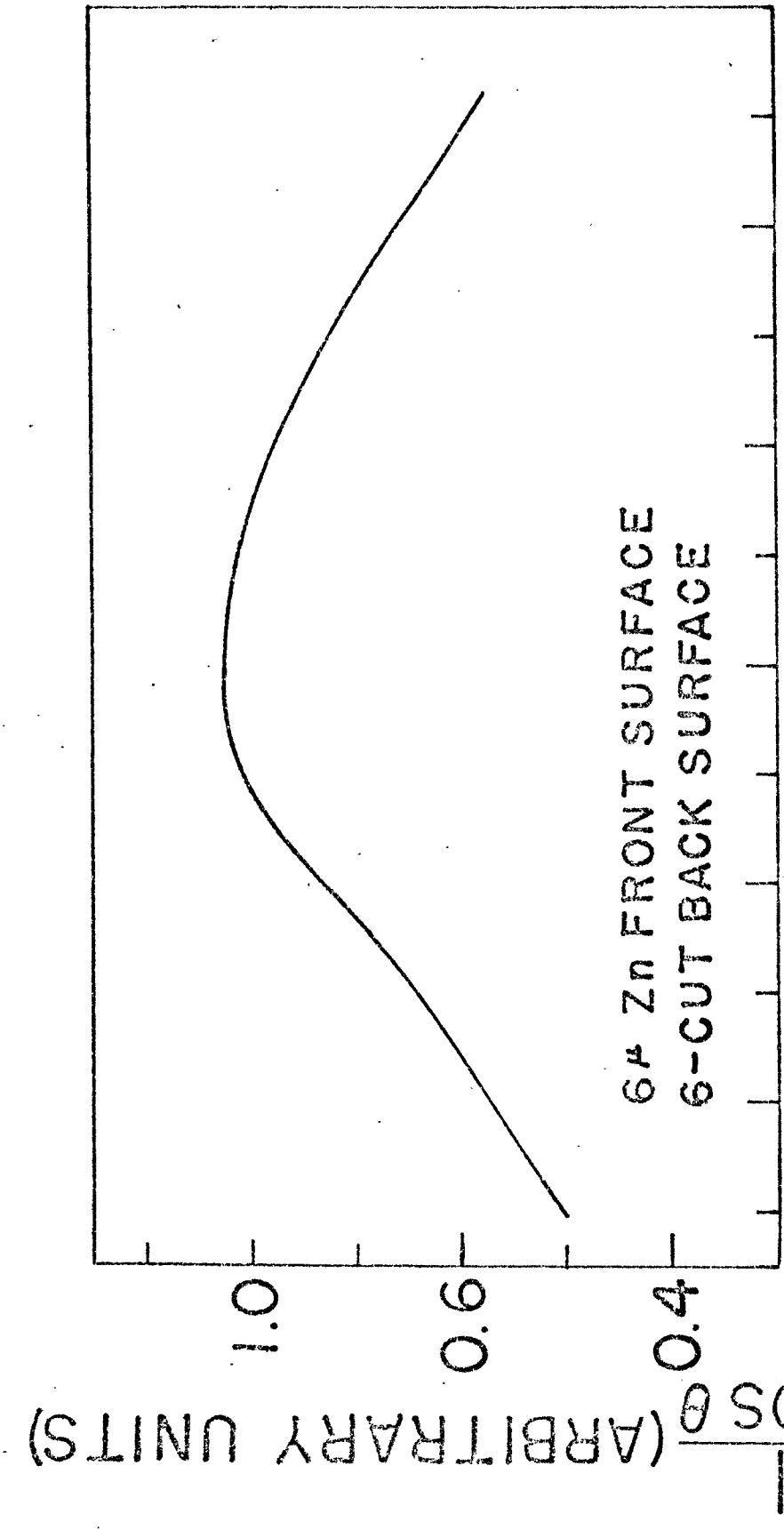

Fig. 14--$\frac{|\rho_{21}|}{\alpha(\theta)\cos\theta}$ vs. angle from hexagonal axis.

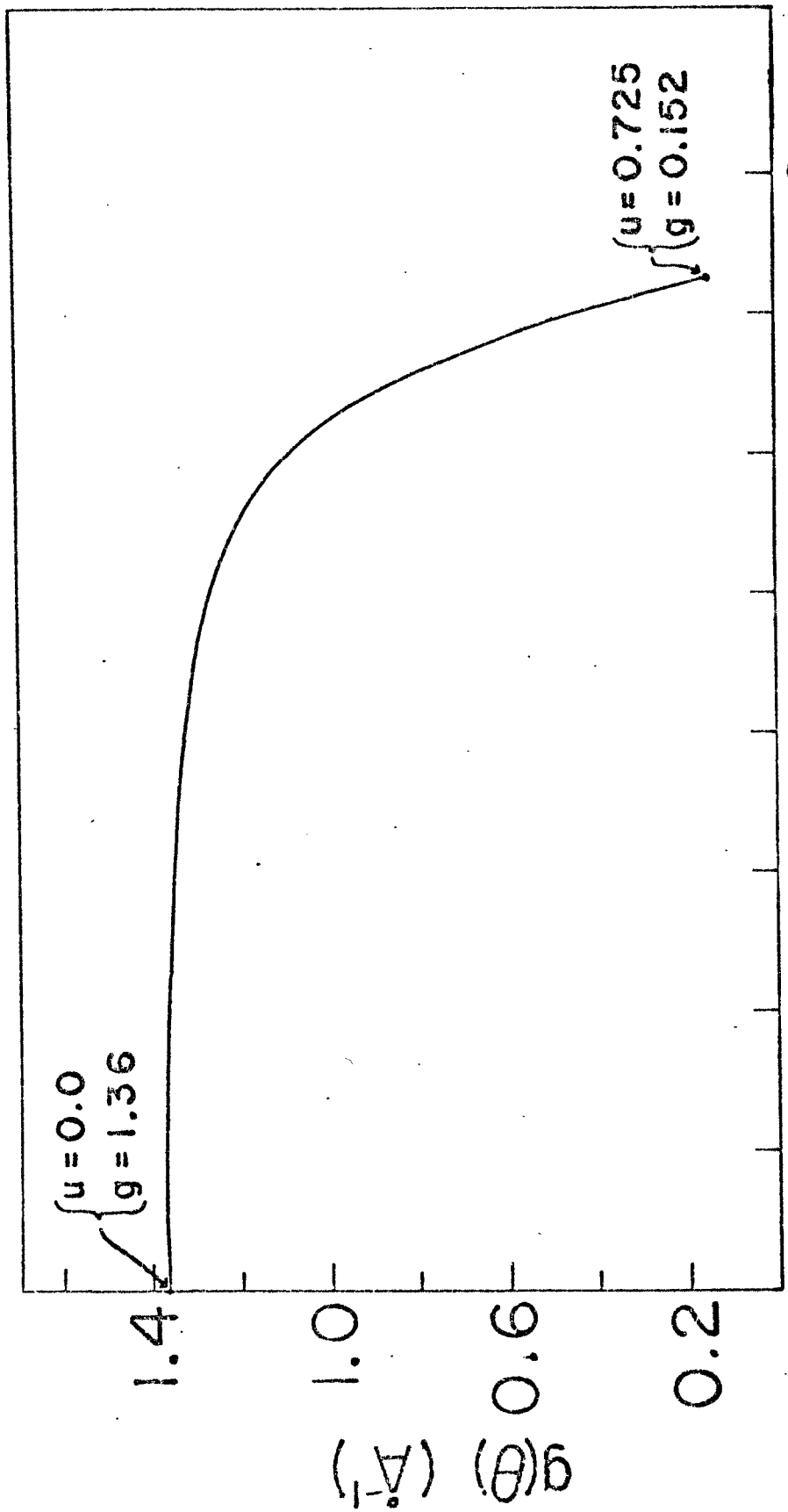

Fig. 15--Gaussian radius of curvature of Fermi surface vs. u

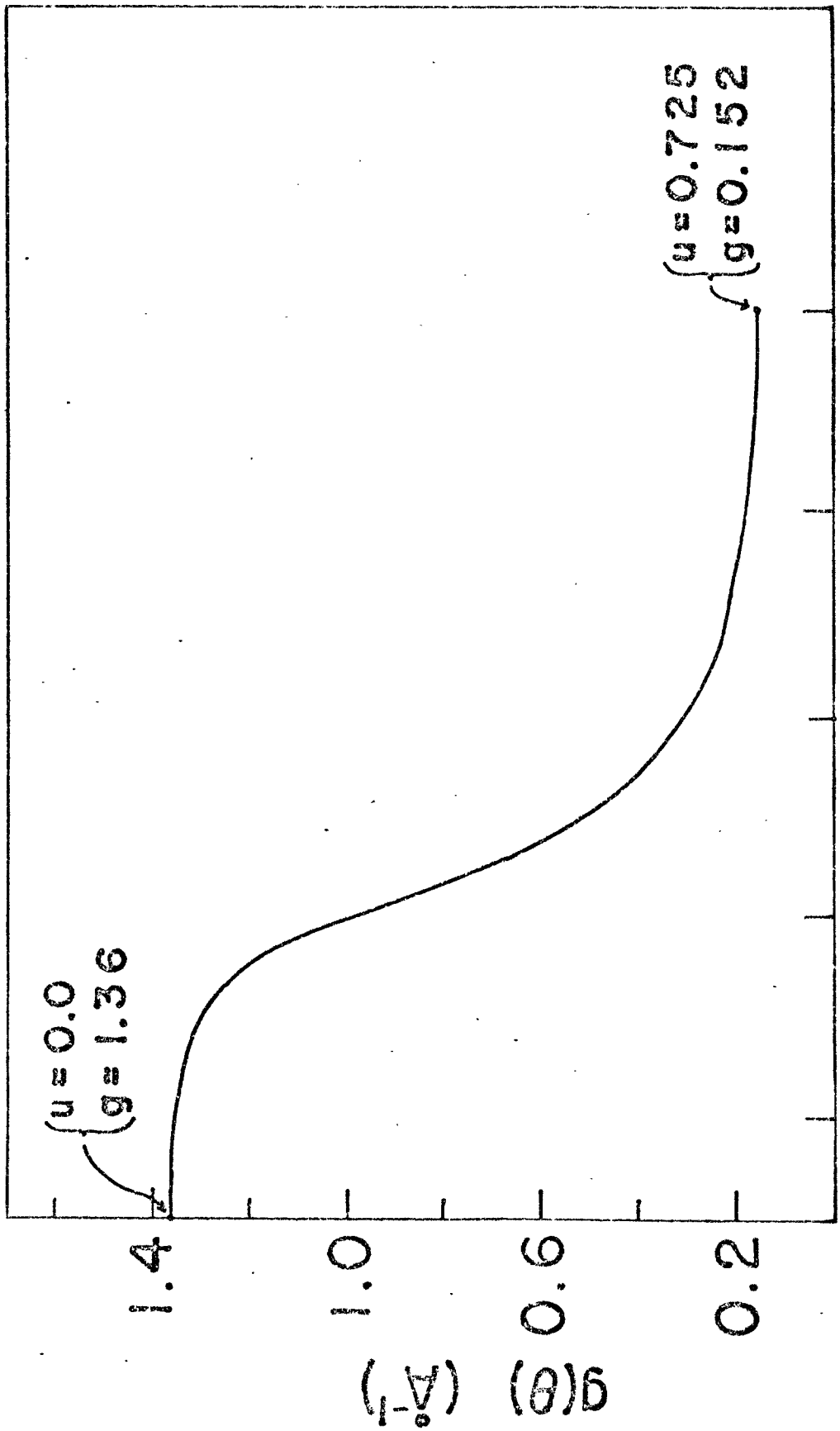

Fig. 16--Gaussian radius of curvature of Fermi surface vs. angle from hexagonal axis.

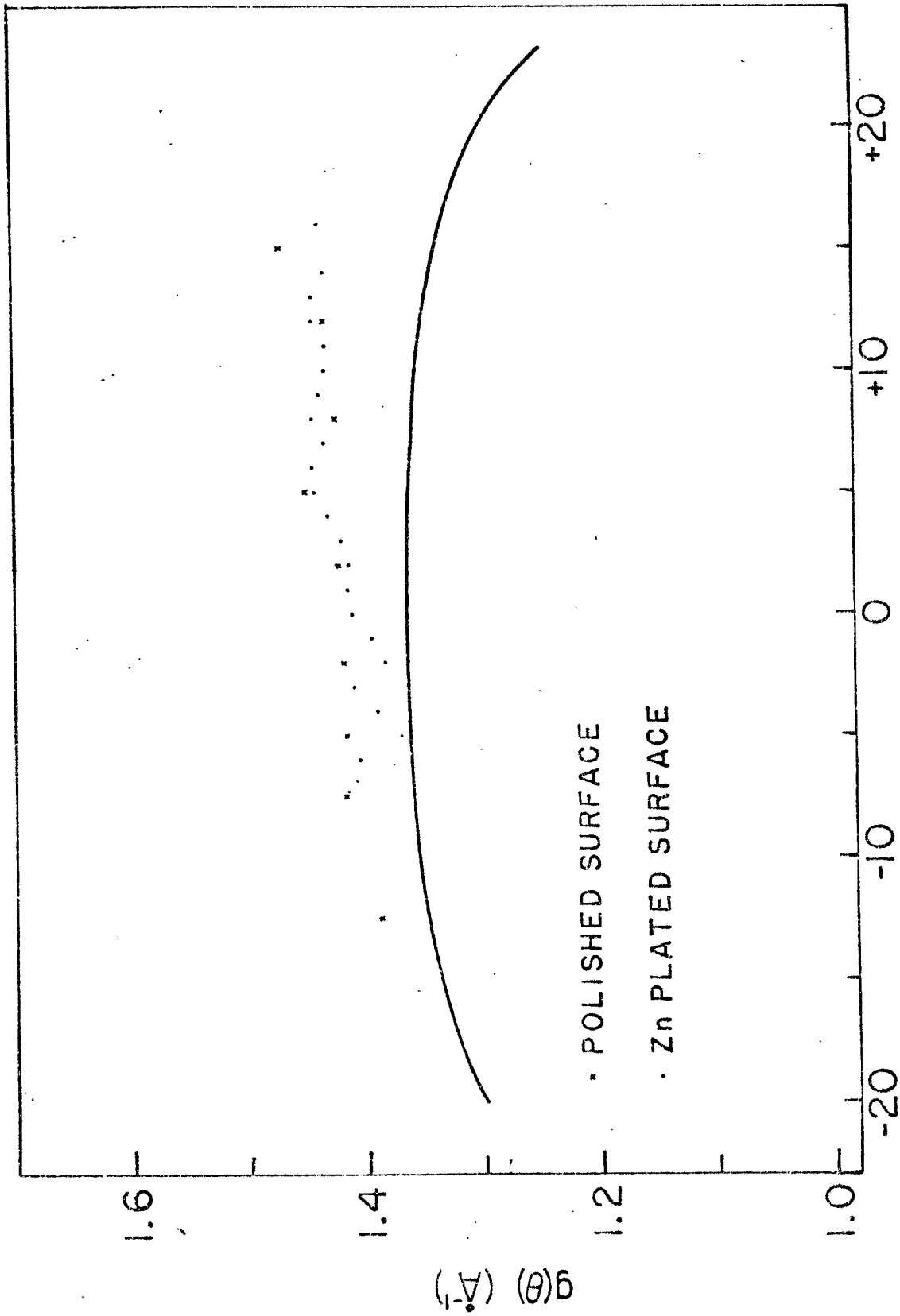

Fig. 17--Experimental values of the Gaussian radius of curvature vs. theoretical values.

BIBLIOGRAPHY

Books

Brimi, Marjorie A. and James R. Luck, Electrofinishing, New York, American Elsevier Publishing Company, Inc., 1965.

Lane, E. P., Metric Differential Geometry of Curves and Surfaces, Chicago, The University of Chicago Press, 1940.

Ziman, J. M., Electrons and Phonons, London, Oxford University Press, 1960.

Articles

Daniel, M. R. and L. MacKinnon, "The Magnetoacoustic Effect and the Fermi Surface of Cadmium," Philosophical Magazine, VIII (April, 1963), 537-552.

Grenier, C. G., K. R. Efferson, and R. M. Reynolds, "Magnetic Field Dependence of the Size Effect in the Transport Coefficients of a Cadmium Single Crystal at Liquid-Helium Temperatures," Physical Review, CXLIII (March, 1966), 406-420.

Gurevich, V. L., "Oscillations in the Conductivity of Metallic Films in Magnetic Fields," Soviet Physics JETP, 8 (March, 1959), 464-470.

Mackey, H. J., J. R. Sybert, and J. T. Fielder, "Magnetomorphic Oscillations in the Hall Effect and Magnetoresistance in Cadmium," Physical Review Letters, XI (September, 1963), 260-264.

Mackey, H. J. and J. R. Sybert, "Harmonic Content of Magnetomorphic Oscillations in the Kinetic Coefficients of Electron Transport due to Partially Specular Boundary Scattering," Physical Review, CLVIII (June, 1967), 658-661.

Mackey, H. J., and J. R. Sybert, "Magnetomorphic Oscillations in Crystals with Two Surface-Scattering Parameters," Physical Review, CLXIV (December, 1967), 982-984.

Sondheimer, E. H., "The Influence of a Transverse Magnetic Field on the Conductivity of Thin Metallic Films," Physical Review, LXXX (November, 1950), 401-406.

Zebouni, N. H., R. E. Hamburg, and H. J. Mackey, "Magnetomorphic Oscillations in the Hall Effect and Magnetoresistance in Cadmium," Physical Review Letters, XI (September, 1963), 260-264.

Unpublished Material

Fielder, James T., "Effect of Sample Geometry on Magnetomorphic Oscillations in the Hall Effect in Cadmium at Liquid-Helium Temperatures," unpublished master's thesis, Department of Physics, North Texas State University, Denton, Texas, 1966.